

# A Study of Inter-Crystal Scatter in Small Scintillator Arrays Designed for High Resolution PET Imaging

Yiping Shao, Simon R. Cherry, Stefan Siegel, Robert W. Silverman  
 Crump Institute for Biological Imaging, Department of Molecular and Medical Pharmacology,  
 UCLA School of Medicine, Los Angeles, CA

## Abstract

Inter-crystal scatter causes mispositioning of scintillation events, which is of particular concern in imaging detectors based on small discrete scintillator elements. Because it is difficult to measure the scatter and its effects on detector intrinsic spatial resolution, a Monte Carlo simulation has been used to study inter-crystal scatter effects for evaluating and optimizing the design of a high resolution animal PET detector based on an array of small scintillator crystals. In this simulation, we quantitatively assess the mispositioning of events due to inter-crystal scatter as a function of parameters such as different scintillator materials, crystal geometry,  $\gamma$  ray incident angle and applied energy threshold. In analyzing the tradeoff between the detector efficiency and the position detection accuracy, we found that the mispositioning is not sensitive to the energy threshold, however it does change rapidly with the crystal length and the gap between crystals. We also compared four different crystal positioning algorithms to provide a theoretical estimate of positioning accuracy and to determine the best algorithm to use. To study how inter-crystal scatter affects detector spatial resolution, we analyzed the coincidence line spread function with and without inter-crystal scatter and found that the inter-crystal scatter had very little effect on the FWHM and FWTM of the coincidence line spread function.

## I. INTRODUCTION

In order to achieve high spatial resolution positron emission tomography (PET), particularly for scanners dedicated to small animal imaging, a detector which comprises an array of small scintillators with one-to-one coupling to the photon detector offers many attractive features [1-3]. However, as the dimensions of the discrete scintillator elements reduce to satisfy spatial resolution requirements,  $\gamma$  ray inter-crystal scatter will increase and the corresponding crystal mispositioning may have a direct impact on detector intrinsic resolution. In designing and developing a high resolution gamma ray imaging detector, it is therefore important to understand how the detector spatial resolution is affected by factors such as crystal length, cross section size, spacing between crystals, incident angle and scintillator material, not only by photoelectric interactions but by Compton scatter interactions as well.

Since it is virtually impossible to directly measure Compton scatter distributions in small scintillator arrays experimentally, particularly at 511 keV, where achieving collimated beams less than 1 mm is difficult, we turned to Monte Carlo simulations to investigate the inter-play between

inter-crystal scatter and factors related to array geometry, energy threshold and positioning schemes. We also compared positioning accuracy for bismuth germanate (BGO) with that obtained with lutetium oxyorthosilicate (LSO), a new scintillator which looks particularly promising for PET applications [4].

## II. VALIDATION OF THE SIMULATIONS

The simulations are based on the calculation of the probability of photoelectric or Compton interactions at different gamma ray energies. The location, scatter angle and energy deposited at each interaction is recorded. The propagation of scintillation light photons generated in the crystal is calculated using DETECT [5]. All simulations in this study assume crystal surfaces are mirror polished except the one opposite to the photodetector which has a rough surface [6]. The crystals were simulated as being wrapped in a diffuse external reflector with 98% reflectivity.

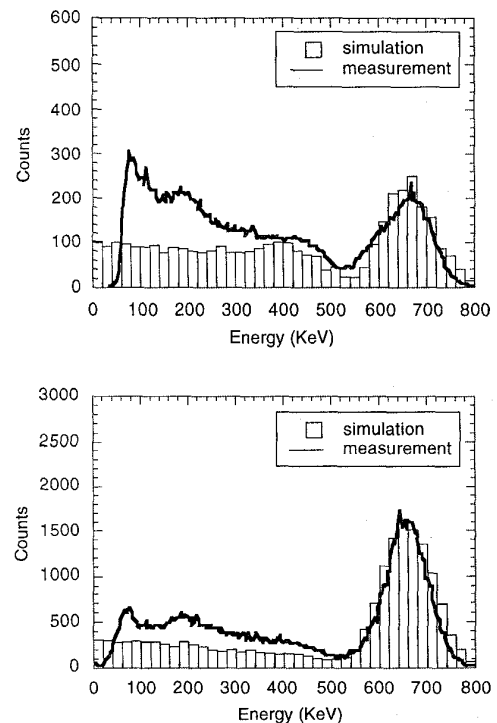


Fig. 1 A comparison of simulated and measured energy spectra for BGO crystals of different sizes irradiated with a 662 keV source: 2x2x10 mm (top) and 12x14x25 mm (bottom).

To validate the simulation code, we checked the distribution of the scatter lengths, deflection angles and energy loss the code provided to ensure that they agreed with theoretical distributions. In addition, the simulated energy spectra were compared with experimental measurements for two very different size BGO crystals, as shown in Fig. 1. Experimentally, the BGO crystals had the same surface treatment as in the simulations and were wrapped with white teflon tape. A 662 keV  $\gamma$  ray flood source irradiated the crystal which was directly coupled to a PMT. The peak-to-valley ratios and the peak shapes demonstrate good agreement between simulations and measurements. The discrepancy in the low energy region, which is much smaller in the case of large crystal, is mainly due to background scatter from supporting structures and electronic noise in the measurement.

To verify the code for inter-crystal scatter, we first measured the energy spectrum from an individual 2x2x10 mm BGO crystal with a 662 keV flood source. We then placed that crystal at the center of a 3x3 array of 2x2x10 mm BGO crystals and irradiated the whole array, while only measuring the energy spectrum from the central crystal. In this way, we measured the effects of inter-crystal scatter from the surrounding scintillator crystals into the crystal of interest (Fig. 2). Simulations were then performed for the same geometries. Both the measurements and the simulations show similar increases in Compton scatter in the array relative to the individual crystal.

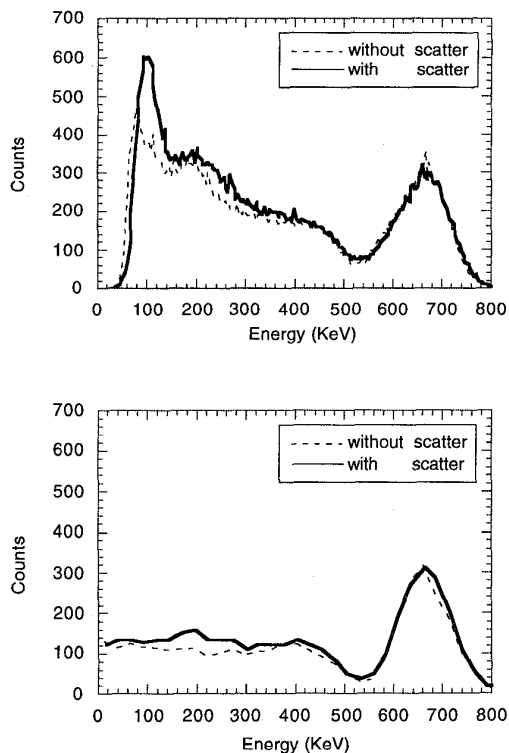


Fig. 2 Energy spectra from a small 2x2x10 mm BGO with and without inter-crystal scatter from measurements (top) and simulations (bottom).

### III. POSITION DETECTION ACCURACY

These simulations focus on an 8x8 array of 2x2x10 mm crystals, which is the current design we are pursuing for a high resolution gamma ray imaging detector for a dedicated small animal PET (microPET) [1]. The Monte Carlo simulation starts with 511 keV gamma rays irradiating one crystal in the scintillator array with a certain incident angle. The distribution of all interaction locations and corresponding energy losses are then stored for crystal identification. Fig. 3(a) represents a simulation of the irradiation of one crystal in the BGO array and shows the distribution of all interaction locations in the plane perpendicular to the crystal height. After scintillation photon propagation, a positioning scheme is chosen to identify the crystal of interaction. For instance, the signal weighted centroid of the interaction location of each event in Fig. 3(a) is calculated and is shown in Fig. 3(b).

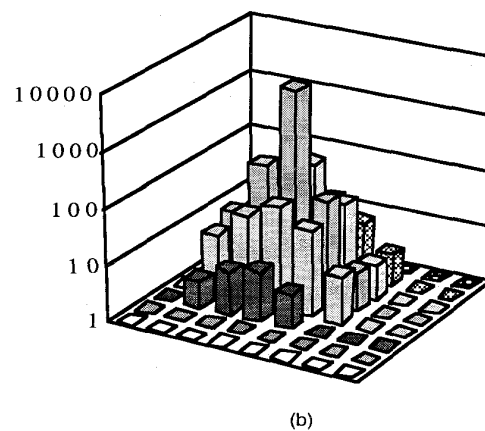
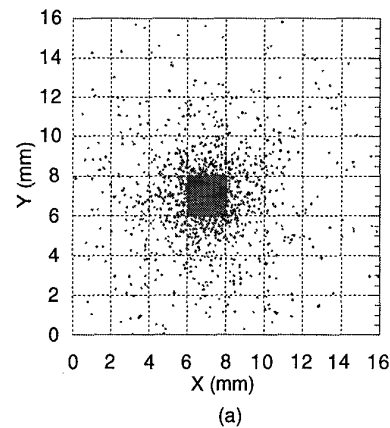


Fig. 3 (a) A scatter plot of the location of interactions from a 511 keV source irradiating a central crystal within an 8x8 array of 2x2x10 mm BGO. (b) The distribution of event centroids calculated by weighting the signals from the same data set. A log vertical scale is used.

To quantitatively assess the effects of inter-crystal scatter, we define *position detection accuracy* as the percentage of events which are correctly positioned in the crystal that is irradiated. Therefore, this quantity measures the accuracy of crystal identification. Several parameters which affect the position detection accuracy were studied in these simulations for both BGO and LSO scintillator materials.

### A. Crystal Positioning Scheme

Based on the intensity of scintillation light collected and the distance from the interaction location to the bottom of the crystal (the side which is connected to the photo detector), as schematically shown in Fig. 4, several different positioning schemes can be defined for events which undergo inter-crystal scatter:

- **weighted energy:** the crystal of interaction is determined by finding the centroid which is weighted by each interaction intensity in the plane perpendicular to the crystal height. This is essentially the scheme being used in the conventional PET block detector [7], and it can be easily implemented in several different ways without requiring individual channel readout, for example by using simple charge division readout methods [8].

- **maximum energy:** the crystal of interaction is defined as the crystal with the maximum intensity. This scheme requires a detector with individual channel readout.

For a detector with individual channel readout and depth of interaction measurement capability (see [2] for example), two additional positioning schemes can be defined by the distance  $Z$ , the distance from an interaction location to the bottom of the crystal.

- **maximum  $Z$ :** The crystal of interaction is defined as the crystal containing an interaction with the largest  $Z$ .

- **minimum  $Z$ :** The crystal of interaction is defined as the crystal containing an interaction with the smallest  $Z$ .

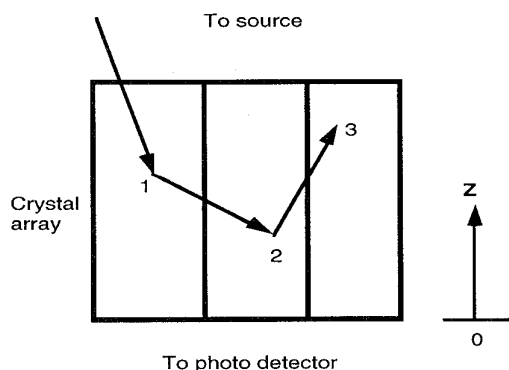


Fig. 4 Schematic drawing showing multiple interactions in crystal array and the definition of distance  $Z$ .

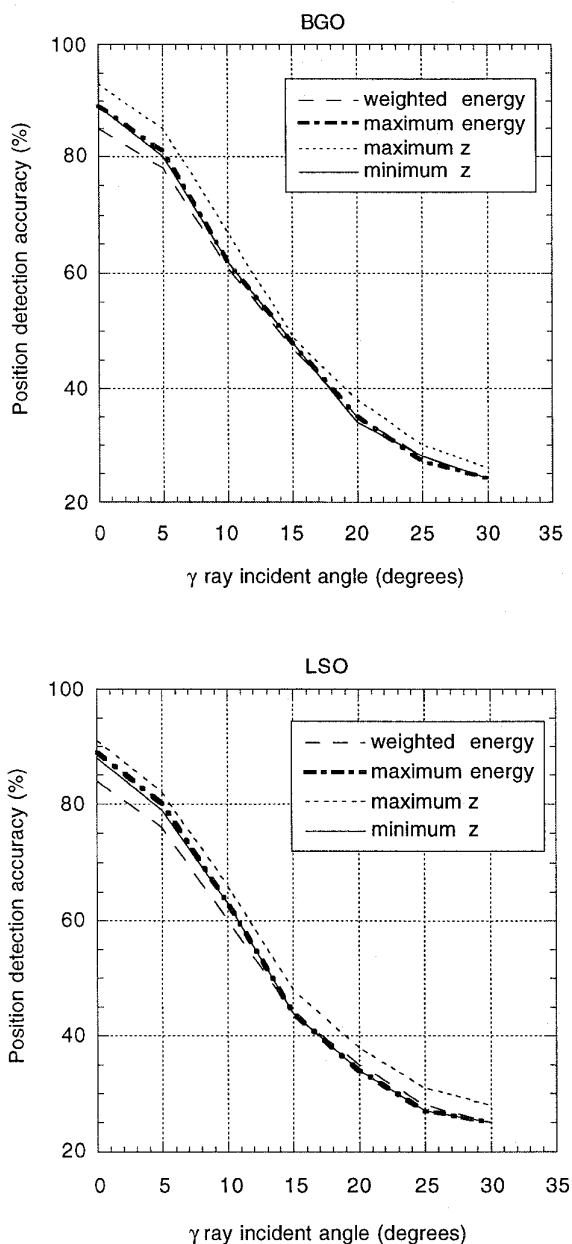


Fig. 5 Position detection accuracy for several crystal identification schemes for different  $\gamma$  ray incident angles. A 511 keV source irradiated a central crystal of an  $8 \times 8$  array of  $2 \times 2 \times 10$  mm scintillators. There is no energy threshold applied.

The simulations were performed for an  $8 \times 8$  array of  $2 \times 2 \times 10$  mm crystals with a 0.25 mm gap (assuming zero interaction probability inside the gap) between crystals. A 511 keV gamma ray source irradiated one central crystal and different positioning schemes were applied to the data for crystal identification. Fig. 5 illustrates that for both BGO and LSO

the maximum Z scheme yields the highest position detection accuracy, while the weighted energy scheme leads to the worst position detection accuracy. The difference between all schemes is less than 10%. It also shows that the position detection accuracy decreases rapidly with increasing gamma ray incident angle, as would be expected.

In evaluating the different positioning schemes, we neglect factors such as energy resolution, depth of interaction resolution and detector signal-to-noise ratio in order to confine the investigation to the mispositioning due purely to the inter-crystal scatter itself. Although these other factors are important in a real scanner, they are detector system parameters and should be studied with the overall performance of the photodetector and electronics. The simulations here provide a basic understanding of the intrinsic effect caused by Compton scatter interactions, which will ultimately be the limiting factor in event positioning in small scintillator arrays.

Since the weighted energy scheme requires less stringent detector capability and is implemented in one form or another in the majority of PET detectors, the following simulations will use this positioning method exclusively.

### B. Crystal Size

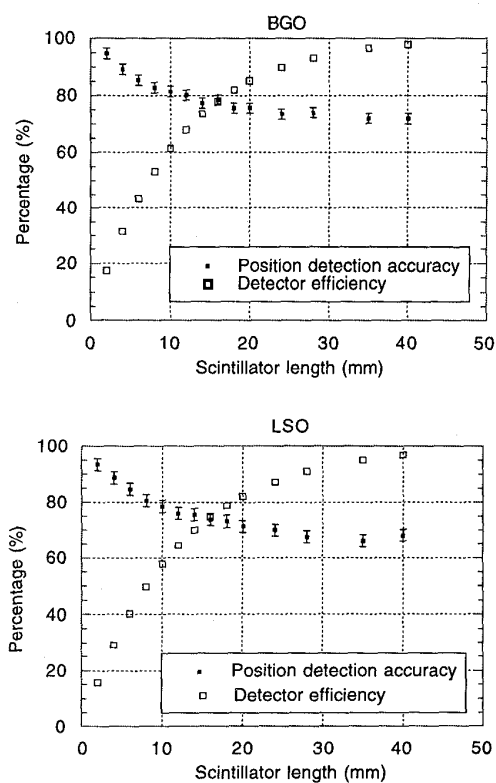


Fig. 6 Position detection accuracy as a function of crystal length. A 511 KeV source with  $0^\circ$  incident angle irradiated a central crystal of an  $8 \times 8$  array of scintillators. No energy threshold is applied.

As the crystal length is increased, an increase in inter-crystal scatter and worse position detection accuracy are expected. Fig. 6 shows both position detection accuracy and detector efficiency as a function of crystal length. This simulation helps to illustrate the difficult tradeoff between detector efficiency and the position detection accuracy. Although LSO has a lower position detection accuracy than BGO because of the lower photoelectric/ Compton interaction ratio (0.78 for BGO versus 0.52 for LSO at 511 KeV), the difference is quite small. For crystal lengths under 15 mm, the difference in position detection accuracy between the two scintillators is less than 3%.

The position detection accuracy as a function of the cross-sectional area is shown in Fig. 7 and reflects the tradeoff between spatial resolution and crystal mispositioning. Even with  $1 \times 1$  mm crystals, the position detection accuracy is still close to 70%. This suggests that very small crystal arrays can be used effectively as a means of obtaining high spatial resolution. The data also provides further evidence that there is very little degradation in position detection accuracy by using LSO in place of BGO.

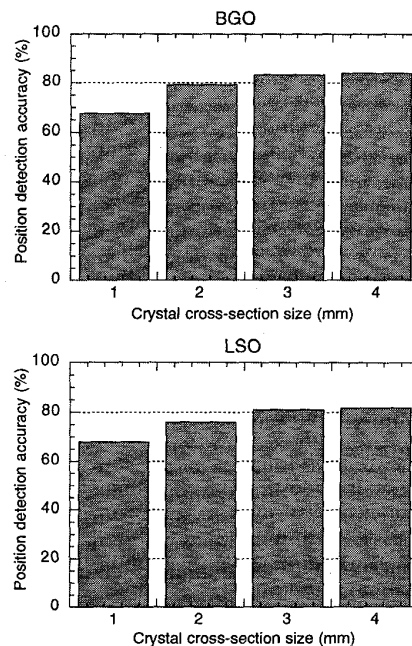


Fig. 7 Position detection accuracy as a function of crystal cross-sectional area. The crystals have a square cross-section shape with a fixed length of 10 mm. A 511 keV source with  $0^\circ$  incident angle irradiated a central crystal in an  $8 \times 8$  array of scintillators.

### C. Gap between Crystals

Using an external reflector is very important to improve the scintillation light collected from a scintillation crystal. However, it leaves a gap between the crystals which affects position detection accuracy and sampling characteristics. In

this simulation, we are only concerned with the gap inside the crystal array, and assume that the probability of gamma ray interaction with the reflector in these gaps is zero. Fig. 8, as an example, shows that the position detection accuracy increases with increasing gap size due to solid angle effects. It indicates that better position detection accuracy can be attained by wider spacing of the array elements, at the expense however of sensitivity and sampling.

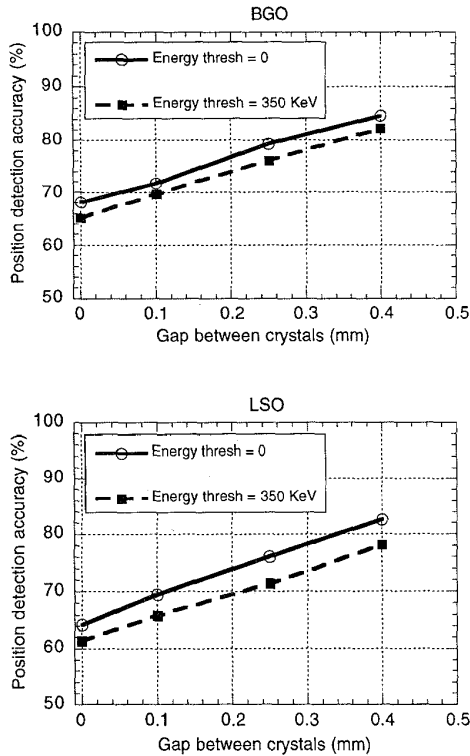


Fig. 8 Position detection accuracy as a function of the gap between crystals. A 511 KeV source with 5° incident angle irradiated a central crystal in an 8x8 array of 2x2x10 mm scintillators.

D. Low Energy Threshold

In Fig. 9, we show the position detection accuracy versus the low energy threshold applied to the data. It is worth noticing that the position detection accuracy decreases as the low energy threshold is increased. Events which undergo multiple interactions within the array, which is the major source of mispositioning, generally deposit a total energy equal or close to 511 keV, and therefore are not affected much by the lower energy threshold. Events which undergo a single Compton interaction, which yield the correct crystal identification, deposit less than 511 keV energy and are affected by the lower energy threshold. Due to the fact that events with a single Compton interaction are a small fraction of the total events, the position detection accuracy decreases quite slowly.

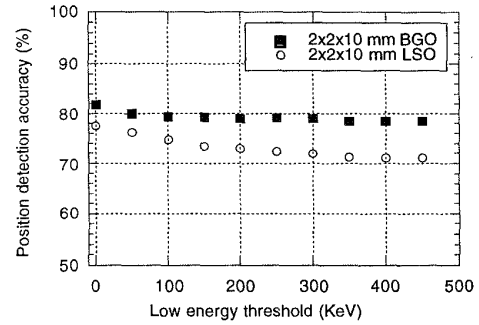


Fig. 9 Position detection accuracy as a function of low energy threshold. A 511 KeV source with 0° incident angle irradiated a central crystal in an 8x8 array of 2x2x10 mm scintillators.

IV. COINCIDENCE LINE SPREAD FUNCTION

Although inter-crystal scatter can cause mispositioning of events, it is not clear how this may affect spatial resolution as characterized by the coincidence line spread function (CLSF). In this simulation, we studied the CLSF at a central location between a pair of detectors. Each detector consists of an 8x8 array of 2x2x10 mm scintillator crystals with 0.25 mm gap between adjacent crystals. The separation between the two detectors is 17.2 cm and a total of 20,000 positron-electron annihilation events were simulated at each position as the source was stepped between the detectors in 0.2 mm increments. The geometrical set-up reflects the design of the microPET detectors and system [1].

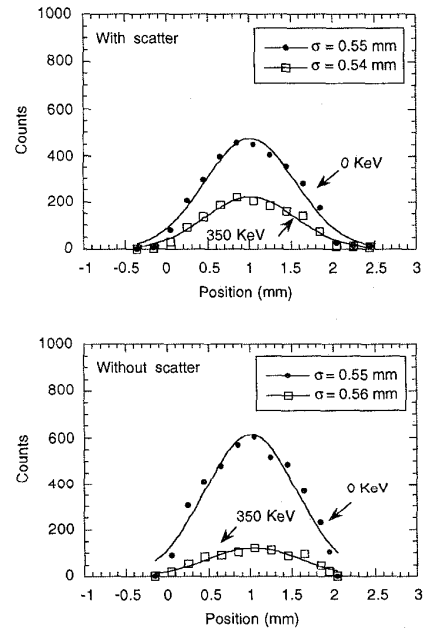


Fig. 10 Coincidence line spread function (BGO) with inter-crystal scatter (top) and without scatter (bottom). Gaussian curves were used to fit the simulated points with different low energy threshold applied.

Figs. 10 and 11 show the simulated CLSF's with and without inter-crystal scatter for BGO and LSO respectively. Fitting a Gaussian function to the CLSF distributions yields a FWHM ranging between 1.22 and 1.32 mm ( $\text{FWHM} = 2.35 \times \sigma$ ) for the  $2 \times 2 \times 10$  mm scintillator array. Interestingly, detector intrinsic spatial resolution does not appear to be adversely affected by inter-crystal scatter and there is no significant difference between using BGO and LSO. Similar results are also obtained from simulations using other array geometries. These results suggest that inter-crystal scatter, when viewed in *coincidence*, has a similar spatial distribution to unscattered events. This is due to the high probability of small angle forward scatter and the reduction in mispositioning in a coincidence set-up relative to a singles set-up.

These simulations of the CLSF demonstrate good agreement with experimental measurements using two micropET detectors. The simulations predict a CLSF with 1.3 mm FWHM, while the experimental measurement gives 1.4 mm FWHM after correcting for source size [1].

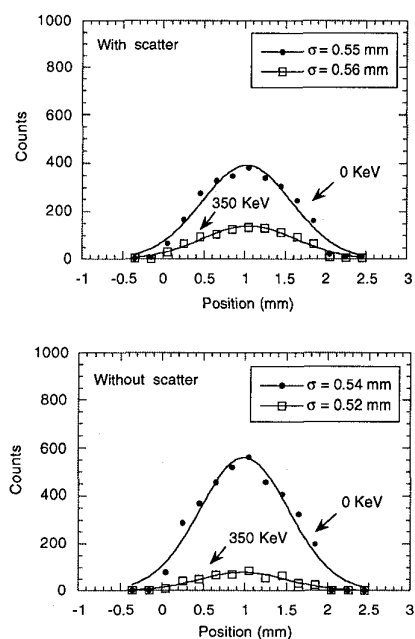


Fig. 11 Coincidence line spread function (LSO) with inter-crystal scatter (top) and without scatter (bottom). Gaussian curves were used to fit the simulated points with different low energy threshold applied.

## V. PARALLAX ERROR

We have also studied how inter-crystal scatter affects parallax errors, which degrades spatial resolution at off-center locations due to detector penetration of oblique gamma rays. The simulations were performed for a pair of  $8 \times 8$  arrays of  $2 \times 2 \times 10$  mm scintillator crystals. The ring diameter was assumed to be 17.2 cm. Simulation results are shown in Figs. 12 and 13 for two incident angles of  $15^\circ$  and  $30^\circ$  respectively. Once again the shapes of the distributions are

quite similar suggesting that inter-crystal scatter has very little effect on spatial resolution.

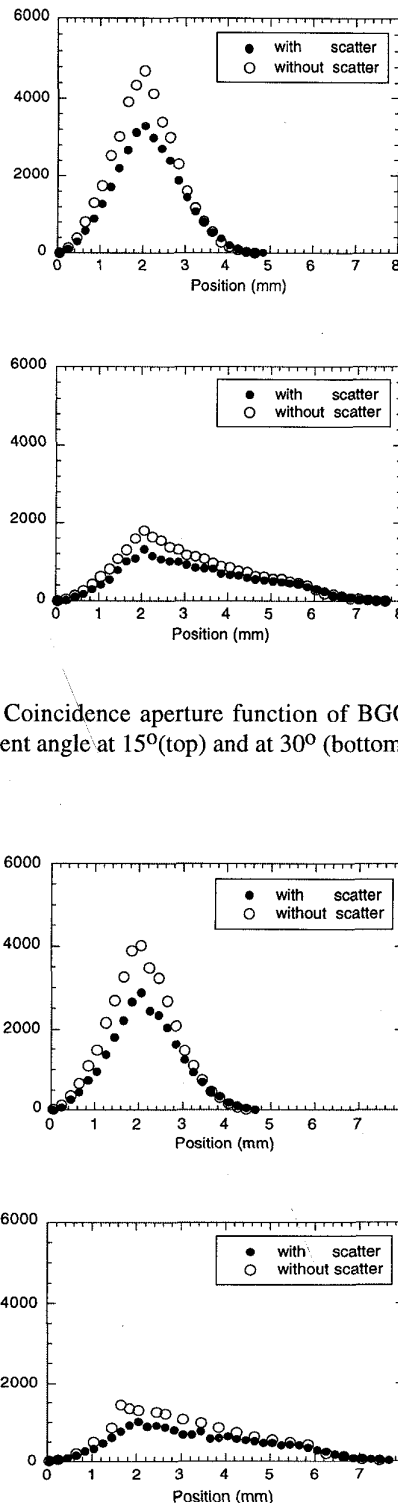


Fig. 12 Coincidence aperture function of BGO with  $\gamma$  ray incident angle at  $15^\circ$  (top) and at  $30^\circ$  (bottom).

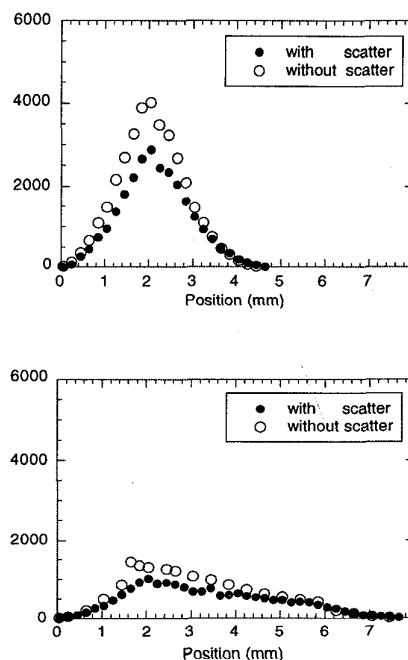


Fig. 13 Coincidence aperture function of LSO with  $\gamma$  ray incident angle at  $15^\circ$  (top) and at  $30^\circ$  (bottom).

## VI. CONCLUSIONS

We have studied the effects of inter-crystal scatter in small scintillator arrays for application in high resolution PET using validated simulations. We have shown that:

- Considering inter-crystal scatter only, the maximum Z positioning scheme yields the highest position detection accuracy, while the weighted energy scheme leads to the worst position detection accuracy.

- Position detection accuracy increases with decreasing length of scintillator or increasing size of scintillator. However, the accuracy is still almost 70% at small incident angle, even for crystals as small as 1x1x10 mm.

- Increasing the energy threshold does not help to reduce crystal mispositioning (although it obviously will help to reject object scatter). There is in fact a trend for decreasing position detection accuracy with increasing low energy threshold.

- LSO has slightly decreased performance in position detection accuracy compared with BGO due to the lower photoelectric cross-section of LSO. The differences are smaller than might be expected - an important result when considering the significant advantage of LSO over BGO, i.e. faster and more light output.

- Inter-crystal scatter has very little effect on the FWHM or FWTM of the coincidence line spread function. If there are any differences, they are in the extremes of the tails of the distribution, which may cause a degradation in image contrast or other effects, rather than a loss in image resolution.

These simulation results suggest that it is worthwhile pursuing detector designs based on discrete arrays of very small BGO or LSO elements for high resolution PET applications, such as animal imaging or mammography.

## VII. ACKNOWLEDGEMENTS

This work was supported by a grant from The Whitaker Foundation and NIH Training Grant T32-CA09092 (Y.S.).

## VIII. REFERENCES

- [1] S.R. Cherry, Y. Shao, S. Siegel, R.W. Silverman, "Optical fiber readout of scintillator arrays using a multi-channel PMT: A high resolution PET detector for animal imaging," *IEEE Trans. Nucl. Sci.*, 1996 (to be published)
- [2] W.W. Moses, S.E. Derenzo, R. Nutt, "Performance of a PET module utilizing an array of silicon photodiodes to identify the crystal of interaction," *IEEE Trans. Nucl. Sci.*, vol.40, pp.1036-1040, 1993
- [3] R. Lecomte, D. Schmitt, L. Lamouret, "Geometry study of a high resolution PET detection system using small detectors," *IEEE Trans. Nucl. Sci.*, vol.31, pp.556-561, 1984
- [4] C.L. Melcher and J.S. Schweitzer, "Cerium-doped lutetium oxyorthosilicate: A fast, efficient new scintillator," *IEEE Trans. Nucl. Sci.*, vol.39, pp. 502-505, 1992.
- [5] G.F. Knoll, T.F. Knoll, T.M. Henderson, "Light collection in scintillating detector composites for neutron detection," *IEEE Trans. Nucl. Sci.*, vol.35, pp.872-875, 1988
- [6] S.R. Cherry, Y. Shao, S. Siegel, R.W. Silverman, "Collection of scintillation light from small BGO crystals," *IEEE Trans. Nucl. Sci.*, vol.42, pp.1058-1063, 1995
- [7] M.E. Casey and R. Nutt, "A multicrystal two dimensional BGO detector system for positron emission tomography," *IEEE Trans. Nucl. Sci.*, vol.33, pp. 460-463, 1986.
- [8] S. Siegel, R.W. Silverman, Y. Shao, S.R. Cherry, "Simple charge division readouts for Imaging Scintillator Arrays using a Multi-Channel PMT," in: Conf. Record of the 1995 IEEE Nuclear Science and Medical Imaging Conference, San Francisco, CA